# Estimating the deflection of weft yarn in plain woven fabric using yarn pull out test

Mohammad Ghane[a] & Vhahid Zarezadeh Lari

Department of Textile Engineering, Isfahan University of Technology, Isfahan, Iran

A simple and practical model has been proposed to calculate the deflection of weft in a plain woven fabric using yarn pull out test. In this modeling, the weft yarn is considered as an elastic beam, which is fixed supported at ends, and deflected at the middle by the normal load applied by the warp. The case of small deflection is adopted to calculate the maximum deflection of weft yarn and to study the shape and geometry of the bent weft. The normal load is estimated from pullout test. Bending rigidity of the weft yarn is calculated from the relation between the bending rigidities of fabric and thread. Five different weft densities have been studied. The shape of actual weft has been studied by microscopic photography from the lateral section of the fabric, and compared to the theoretical deflection curve of weft based on small deflection modeling. The results show that the actual and theoretical curves are reasonably close to each other. The maximum deflection of the weft yarn increases as the weft density (picks/cm) increases. This may be due to the increase in normal load in higher densities of the weft yarns. The results also show that the deviation of theoretical curve from the actual curve increases with the decrease in weft density.

**Keywords**: Elastic beam, Fabric rigidity, Plain woven fabric, Pullout force, Weft deflection, Weft density

## 1 Introduction

The study of fabric structure was first started by Pierce, proposing some geometric modeling of yarn in the fabric. Different theories and models were later presented by researchers regarding the bending of yarn in fabric[1]. These theories are based on the Pierce theory. Considering the yarn as an elastic beam, its deflection in fabric is affected by two main parameters, viz yarn rigidity and normal load applied on the weft through warp.

Yarn deflection in fabric, which is due to the interaction of threads, can influence many properties of fabric. Yarn deflection in the fabric depends on fabric and yarn geometry[2] and the bending behavior of the yarns. It can affect many characteristics of the fabric. For example, such surface properties of the fabric as yarn protrusion, friction and touch could be influenced by thread deflection in the fabric. Thread deflection also affects visual properties of the fabric surface such as light reflection, luster and roughness[3]. Mechanical performance of the fabric depends largely on the geometry and shape of thread deflection.

Study and measurement of yarn rigidity and bending of yarn in fabrics has been a major subject in previous studies and investigations. Wei and Chen[4] used the Pierce geometric model and Grossberg's two-region model to calculate the ratio of bending rigidity of fabric to yarn. Lomov *et al.*[5] used the elastica and energy method and calculated the ratio of fabric-to-yarn rigidities. Ghosh and Zhou[6] studied the characterization of fabric bending and reviewed the principles of bending measurements. Cantilever beams were also used to model the bending behavior of yarns[7].

Estimation of normal load is useful for predicting deflection of weft yarn in fabric. This is usually obtained from pullout test. Estimation of pullout force has been carried out by different researchers[8,9]. Seo *et al.*[10] estimated the normal load using the modulus of fabric and yarns. Realff *et al.*[11] used a micromechanics model to study the deflection of yarn in fabric structure. They presented a linear relation between the deflection of yarn and the normal load. Stick-slip behavior of para-aramid fabrics in yarn pullout test was studied extensively by Bilisik[12,13].

In the present work, a fixed-fixed elastic beam was considered for the deflection of weft yarn in plain

---
[a]Corresponding author.
E-mail: m-ghane@cc.iut.ac.ir

woven fabric. The weft was assumed fix supported in both ends and deflected in the middle by the normal load exerted by warp. The normal load was calculated using pullout force method. The rigidity of fabric was measured and rigidity of yarn in fabric was calculated. The theoretical shape of the bent weft, based on the small deflection equations, was then provided. The actual shape of the weft was obtained using microscopic method and compared with theoretical curve.

## 2 Theoretical Consideration

### 2.1 Small Deflection Equation

One method to obtain the small deflection equation is using the geometry of the bent beam as shown in Fig. 1. Consider an element with the length of $dL$ along the beam. It can be shown that:

$$d\phi = \frac{dL}{\rho} \text{ or } \frac{1}{\rho} = \frac{d\phi}{dL} \qquad \ldots (1)$$

The slope of the tangent to the curve is:

$$\tan\phi = \frac{dy}{dx} \qquad \ldots (2)$$

where $\rho$ is the radius of the curvature; and $\varphi$, the angle between the tangent to the curve and x-axis. If the deflection is very small relative to the length of the beam, the angle $\varphi$ (in radian) will be very small and thus $\tan\varphi \approx \varphi$ and $dL \approx dx$. In this case, the deflection will be carried to the small deflection case. The curvature of the neutral line ($1/\rho$) is[14]:

$$\frac{1}{\rho} = \frac{d^2 y}{dx^2} = \pm\frac{M(x)}{B} = \pm\frac{M(x)}{EI} \qquad \ldots (3)$$

where bending rigidity ($B$) is equal to the product of elastic modulus ($E$) and moment of inertia of the cross section($I$), i.e. $B = EI$.
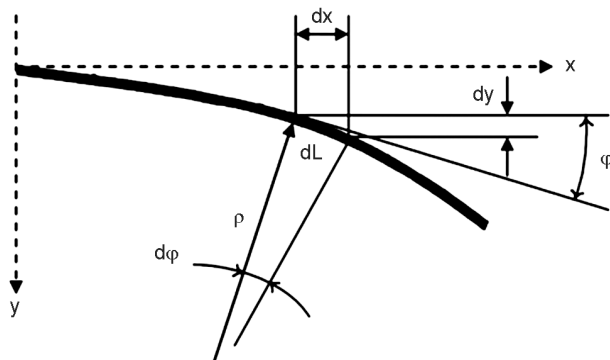
### 2.2 Fixed-fixed Beam Modeling

The beam principles have been used widely to study the bending behavior of textile fabrics[15, 16]. The shape and curve of a bent filament yarn have been studied and the bending rigidity of the yarn is calculated using a fixed-free beam model[17].

In this work, weft yarn is considered as an elastic beam supported at the ends and deflected in the middle by a vertical load. This mechanical model is adopted for a weft yarn in a plain weave fabric, where the weft is assumed to be fixed supported by friction force at intersects and deflected by a normal load inserted by the warp. A schematic diagram of a wave of the bent weft in a plain weave fabric is shown in Fig. 2. The consecutive warps (A and C) are marked at the supports and warp B is marked at the middle of the bent beam. As the tangent to the curve of the deflected weft is equal to zero at points A and C, the deflected weft is assumed to be fixed supported by the adjacent warps (warps A and C in Fig. 2). The distance between the supports is very small (two times the warp spacing) so that the weft can be considered to behave as an elastic beam. The vertical load is applied by the warp B in the middle of warps A and C (Fig. 2). The same model can be considered for the bending of warps deflected by a vertical load applied by wefts.

The assumptions made here to model the deflection of the weft are:

(i) The cross-section of the yarns is assumed to be circular,

(ii) The yarns behave elastically during bending,

(iii) The case of small deflection equations is applied to the model, and

(iv) The vertical load is concentrated on a point in the middle of the deflected yarns.

As seen in Fig. 2, there is a schematic diagram of the central line of the weft modeled as a fixed-fixed
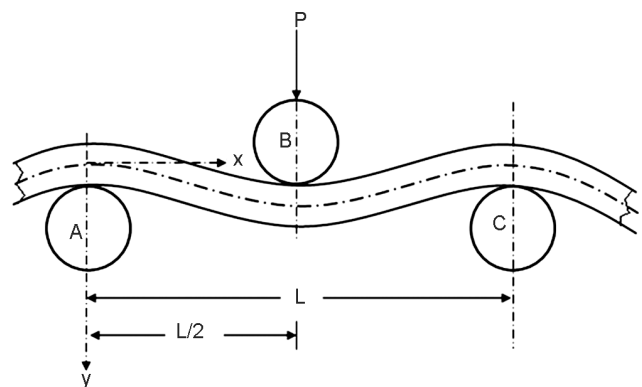


Fig. 1—Schematic representation of bent beam geometry



Fig. 2—Yarn deflection on fixed-fixed beam model

beam deflected in the middle by a concentrated normal load ($P$) in the middle. The centre of coordinate is at the left support. Using the double integration method and boundary conditions, the governing differential equation of the beam can be solved. If the boundary conditions at $x=0$, $y=0$ are applied, the equation of fixed-fixed bent weft is:

$$y = \frac{Px^2}{48B_y}(3L - 4x) \qquad 0 \leq x \leq L/2 \qquad \dots (4)$$

For $L/2 \leq x \leq L$, using two boundary conditions at $x=L$, $y=0$, it can be shown that:

$$y = \frac{P(L-x)^2}{48B_y}(4x - L) \qquad L/2 \leq x \leq L \qquad \dots (5)$$

where $P$ is the normal load (loaded by warp yarn); $L$, the distance between supports (distance between two adjacent warps); and $B_y$, the Bending rigidity of weft yarn.

Applying the model to a bent yarn in a plain weave fabric, we can obtain the maximum deflection in the middle of the bent yarn ($Y_{max}$) in the case of small deflection, as shown below:

$$Y_{max} = \frac{PL^3}{192B_y} \qquad \dots (6)$$

**2.3 Estimation of Normal Load**

As mentioned previously, the formation of fabric during weaving is done at low axial strain of the yams. The normal load $P$ for a fabric at low strain can be estimated using the following formula[10]:

$$\left(\frac{E_f}{E_y}\right)^{2/3} + \left(\frac{P}{2F_s}\right)^2 = 1 \qquad \dots (7)$$

where $E_f$ is the fabric modulus in the weft direction obtained from the stress-strain curve; $E_y$, the weft yam modulus obtained from the stress-strain curve; and $F_s$, the normalized static frictional force, gf/crossing point, obtained from the weft yam pullout force.

**2.4 Rigidity of Yarn in Fabric**

Based on the saw tooth model, Leaf *et al.*[18] used the energy method and presented the following equations:

$$\frac{B_{f1}}{B_{y1}} = \frac{p_2}{p_1(l_1 - 2c_1)} \qquad \dots (8)$$

and

$$\frac{B_{f2}}{B_{y2}} = \frac{p_1}{p_2(l_2 - 2c_2)} \qquad \dots (9)$$

where $B_f$ is the bending rigidity of the fabric per unit width; $B_y$, the bending rigidity of yarn; $c$, the contact length of the yarn at the crossover points; $l$, the modular length; and $p$ the thread spacing which is reciprocal of thread density ($n$). Indices *1* and *2* refer to the warp and weft respectively.

To calculate the contact length ($c$) the contact angle [$\theta$ (radian)] is needed. This can be calculated using the following equations[18] :

$$\theta_1 = 0.185\sqrt{C y_1} \qquad \dots (10)$$

and

$$\theta_2 = 0.185\sqrt{C y_2} \qquad \dots (11)$$

$Cy$ is the crimp percentage of the warp (weft), i.e.

$$Cy_1 = 100 \times (l_1 - p_2)/p_2 \qquad \dots (12)$$

and

$$Cy_2 = 100 \times (l_2 - p_1)/p_1 \qquad \dots (13)$$

Grossberg's suggestion was used to estimate the diameter of the yarn, as shown below:

$$d = 4.44\sqrt{\frac{T_y}{\rho_f}} \times 10^{-3} \qquad \dots (14)$$

where $d$ is yarn the diameter (cm); $T_y$, the linear density of the yarn (tex); and $\rho_f$, the density of the fibers (g/cm$^3$).

Having the yarn diameter and contact angle, the contact length can be calculated from the following equations:

$$c_1 = k_1(d_1 + d_2)\theta_1 \qquad \dots (15)$$

and

$$c_2 = k_2(d_1 + d_2)\theta_2 \qquad \dots (16)$$

where $k$ is the empirical coefficient, assuming that for the circular cross-section shape the value of $k$ is equal to 0.5.

**3 Materials and Methods**

**3.1 Sample Preparation**

In order to study the effect of variation in weft yarn density on yarn protrusion, five plain fabric samples with different weft densities were produced using the air jet Picanol Omniplus weaving machine. The warps and wefts were single yarns with linear density of 19.7 and 29.5 tex respectively. Twist per meter of the

warp and weft yarns were 650 and 580 respectively. The constituent of yarns were 100% cotton produced by a ring-spinning machine.

Samples were produced with five different weft densities, coded as A-E. Other parameters of the weaving machine were kept identical. Reed setting on the weaving machine was the same for all samples. However, some little changes were made in the actual density of warp yarns on the prepared fabric due to variation in weft density. Thus, actual properties of samples were measured using standard methods as shown in Table 1. Using Pierce's model for geometry of plain weave fabrics, different parameters of samples were calculated (Table 2). All samples were conditioned at 21°C and 65% RH. The density of cotton in standard conditions was considered as 1.52 g/cm³. Values of 159.8 and 195.6 μm were calculated for the diameter of warp ($d_1$) and weft ($d_2$) respectively, based on Eq. 14.

### 3.2 Tensile and Pullout Tests

Zwick universal testing machine 1446-60 was used to measure the tensile modulus of fabric and weft yarn. In the case of fabric, 10 samples with width of

Table 1—Properties of samples

| Property | Sample | | | | |
|---|---|---|---|---|---|
| | A | B | C | D | E |
| Warp density ($n_1$), cm⁻¹ | 34.9 | 35.3 | 35.5 | 35.8 | 36 |
| Weft density ($n_2$), cm⁻¹ | 18.2 | 21.3 | 23.9 | 27.2 | 29.7 |
| Fabric thickness ($t$), mm | 0.491 | 0.464 | 0.444 | 0.434 | 0.419 |
| Fabric weight g/m² | 135 | 143 | 152 | 161.5 | 173 |
| Warp crimp ($C_{y1}$), % | 19.76 | 19.84 | 20.16 | 21.04 | 21.84 |
| Weft crimp ($C_{y2}$), % | 7.02 | 7.34 | 8.03 | 8.09 | 10.41 |

Table 2—Fabric parameters calculated by Pierce equations

| Property | Sample | | | | |
|---|---|---|---|---|---|
| | A | B | C | D | E |
| $p_1$, cm | 0.0287 | 0.0283 | 0.0282 | 0.0279 | 0.0278 |
| $p_2$, cm | 0.0553 | 0.0470 | 0.0418 | 0.0368 | 0.0337 |
| $l_1$, cm | 0.0658 | 0.0563 | 0.0503 | 0.0445 | 0.0410 |
| $l_2$, cm | 0.0305 | 0.0304 | 0.0304 | 0.0304 | 0.0307 |
| $\theta_1$, Radian | 0.822 | 0.824 | 0.831 | 0.849 | 0.865 |
| $\theta_2$, Radian | 0.490 | 0.501 | 0.524 | 0.552 | 0.597 |
| $c_2 \times 10^{-4}$, cm | 87.1 | 89.1 | 93.2 | 98.1 | 106.1 |

25 mm were tested. The rate of elongation was 50 mm/min and the gauge length was set to be 150 mm. In the case of weft yarn, 30 samples were tested. The rate of elongation was 50 mm/min and the gauge length was set to be 250 millimeter. Average fabric modulus was obtained from the stress strain curves in N/mm². Average weft yarn modulus ($E_y$) was also obtained from stress strain curves, which is equal to 151.8 cN/tex. Equation (7) was used to calculate normal load. In order to satisfy dimensional compatibility, the unit of fabric modulus must be modified to cN/tex. To obtain this, following equation[19] was used:

$$E_{yf} = \frac{E_f \times t \times w}{T_y \times N} \qquad \dots (17)$$

where $E_f$ is the Fabric modulus in the weft direction (N/mm²); $E_{yf}$, the Modified fabric modulus (cN/tex); $t$, the fabric thickness; $w$, the sample width; $T_y$, the yarn linear density; and $N$, the number of yarns in sample width (tensile test).

Pullout tests of weft yarn were carried out using a Zwick universal testing machine 1446-60. The size of the samples was 50 mm×10 mm. The edges of the samples were fixed in the clamps. The middle weft yarn was then pulled via upper clamp of the machine with speed of 10 mm/min. The length between the fabric upper edge and the stationary upper head of Zwick tester was set to be 60 mm. The yarn free length in the fabric lower edge was 10 mm. These conditions were the same for all samples. As seen in Fig.3, the pull out process contains three different stages. In the first stage, the crimp of the yarn is beginning to straighten (de-crimping) and tensile stress develops in the yarn until the created stress overcomes static friction and the yarn starts to slip. In the second stage, the dynamic friction is involved leading to steak-slip motion and decreasing of pull out force. In the third stage, the yarn comes off the contact points with fabric, leading to sharp decreasing of pull out force.

Based on the curve (Fig. 3) obtained from pullout test, the maximum static friction force ($F_{max}$) between the pulled weft yarn and warp yarn was calculated and then the normalized maximum frictional force ($F_s$) was achieved by dividing $F_{max}$ to the number of crossing points ($N_c$). The values obtained for the normal load, ($P$) are shown in Table 3.
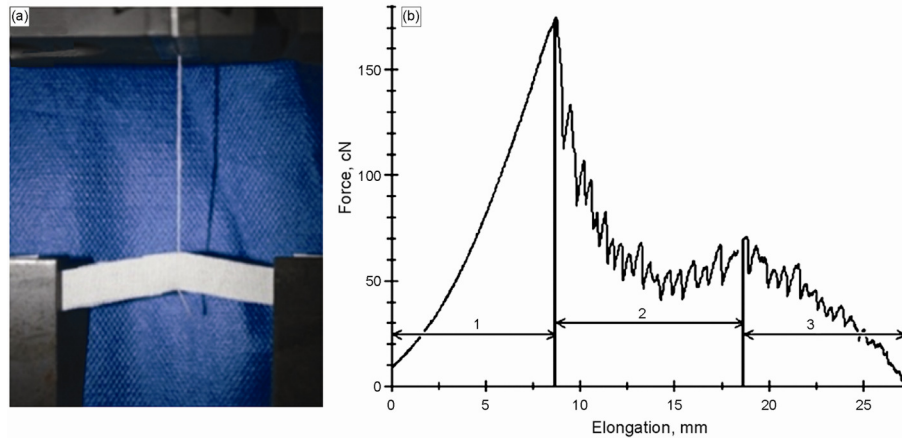
Fig. 3—Force- elongation profile of yarn pullout test [(a) yarn pull out (*in-situ*), (b) force-elongation curve during pull out test]

Table 3—Pullout test results
[Weft yarn modulus ($E_y$) = 151.8 cN/tex]

| Property | Sample A | Sample B | Sample C | Sample D | Sample E |
|---|---|---|---|---|---|
| $E_f$ , N/mm$^2$ | 141.73 | 171.46 | 202.23 | 230.61 | 262.34 |
| Number of yarns in fabric (tensile test , N) | 46 | 53 | 60 | 68 | 75 |
| $E_{yf}$ , cN/tex | 130.3 | 129.2 | 128.9 | 126.7 | 126.2 |
| Samples dimension mm×mm×mm | 50×10×0.491 | 50×10×0.464 | 50×10×0.444 | 50×10×0.434 | 50×10×0.419 |
| Number of crossing points ($N_c$) | 35 | 36 | 35 | 35 | 36 |
| $F_{max}$ , g | 79.43 | 96.30 | 123.95 | 155.64 | 188.90 |
| $F_s$ , g | 2.27 | 2.68 | 3.54 | 4.45 | 5.23 |
| Normal load (P), g | 1.41 | 1.71 | 2.27 | 3.00 | 3.56 |

### 3.3 Bending Test

Bending stiffness of the samples (150 mm×25 mm) was measured using Shirley stiffness tester in weft direction. The amount of the contact length of warp and weft yarns in the intersection points was calculated based on Eqs (10)-(16). Consequently, using Eq. (9), bending stiffness of weft yarn within the fabrics can be calculated. The weft yarn bending rigidity values are shown in Table 4.

### 3.4 Measurement of Weft Deflection

To measure maximum deflection of the weft yarn, cross-sectional images of the fabrics were required. Using a special mold, fabrics were impregnated in an epoxy resin (FK20) with a ratio of 1:2. The set was then cured for 48 h. The resin penetrates deeply into the fabric spaces, making a solid structure after curing. This is necessary as it can prevent the threads from sliding aside during the cutting process and make microscopic observations of the samples possible. Then, the sample was removed from the mold and placed in a microtome cutter machine SLEE MAINZ – Microtec – Cut 4055. The warps and wefts were along the horizontal and vertical directions respectively. To observe the weft wave clearly, cutting was done in the weft direction and the surface of the molded sample was polished. The microtome was adjusted to cut 30 µm thick layers. The cuttings were viewed under a microscope (×100) equipped with a closed circuit camera which was connected to a computer. Special software on the computer, allowed the researchers to calculate any real distance on the object from the images by defining the magnification of the microscope (×100) for the software. Ten samples were examined and the average values of the maximum deflection were calculated and reported for each fabric type (Table 4). Figure 4 shows typical images of the weft wave in the actual fabric.

### 4 Results and Discussion

Pull out test is performed as explained previously (Fig. 3a). After de-crimping, which consumes a little

Table 4—Bending properties of samples in weft direction

| Property | Sample | | | | |
|---|---|---|---|---|---|
| | A | B | C | D | E |
| $B_{f2} \times 10^{-6}$, kg.cm | 8.492 | 11.407 | 14.616 | 19.080 | 23.527 |
| $B_{y2} \times 10^{-6}$, kg.cm$^2$ | 0.217 | 0.238 | 0.256 | 0.266 | 0.270 |
| Beam length (L), μm | 595 | 595 | 590 | 585 | 585 |
| $Y_{max}$(theoretical), μm | 71.29 | 78.82 | 94.85 | 117.61 | 137.48 |
| $Y_{max}$(actual), μm | 84.02 | 94.39 | 110.00 | 126.56 | 141.83 |



Fig. 4—Cross-section of fabrics in weft-wise direction (Sample D)



Fig. 5—Typical diagram of the weft yarn deflection versus the distance (L) between the two supports (Sample D)

force when compared with the fabric deformation, the force *F* is increased to a maximum value ($F_{max}$), which is called the maximum static friction force. Based on the data of the maximum pullout point (Fig. 3b), the static friction force is calculated.

In order to confirm the validity of the small deflection equations, the shape of the actual bent weft in the fabrics was compared with the theoretical curve. The theoretical curves of a bent beam, under conditions identical to those of the deflected weft, were plotted according to equations proposed by the small deformation model [Eqs (4) and (5)], as can be seen in Fig. 5. It is observed that the maximum deflection of weft yarn is in the middle, i.e. *x=L/2*. Using the appropriate software, the *x-y* co-ordinations of some of the points were extracted from the actual curve of the outermost layer of the weft. Based on the experimental data, the actual curves of weft yarn deflection were obtained. A typical graph of theoretical and actual curves is depicted in Fig. 5. The values of the maximum weft yarn deflection for theoretical and actual models are listed in Table 4.

The results show that the actual deflection curve of weft yarn in the fabric is significantly close to the theoretical model for the elastic beams in conditions of small deformation. The deviation of actual curve from the theoretical small deflection curves increases with the decrease of the weft density. The reason for this may be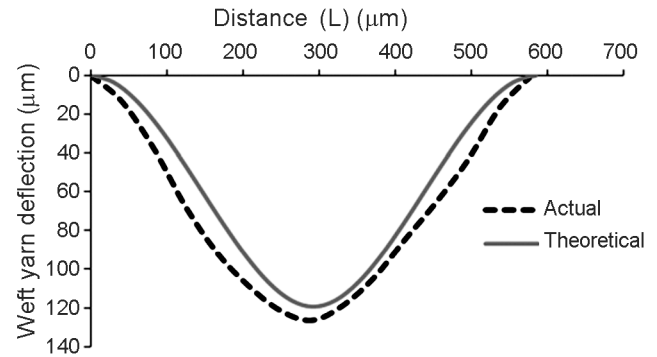 found in the friction force in the cross over points. As mentioned previously, the weft yarn is assumed fix supported at the ends by the friction force in the crossover points. Decrease in weft yarn density leads to decrease in friction force in crossover points. In other words, any slippage or loose contact deteriorates the fixed-fixed supports assumption. This, in return, may lead to more deviation in theoretical model from the experiment curve.

The results also show that the maximum deflection increases with increasing the weft density. To explain this, Eq. (6) must be considered. According to this equation, two opposite trends are observed. First, the maximum deflection is directly related to the normal load P. According to the results, as the density of the weft yarns increases, the normal load also increases (Table 3) leading to the increase of maximum deflection. On the other hand, Eq. (6) shows a reverse relation between the rigidity of yarn and maximum deflection. Table 4 shows that the increase in effective weft yarn rigidity along with the increase in weft density cause the reduction in maximum deflection. However, the resultant effect is the increase in maximum deflection with the increase in weft density.

It can be concluded that the effect of normal load is larger than that of rigidity of the weft yarn. Another point that can be explained in this context is the yarn flattening during weaving. The cross-section of the bent weft deviates from circular shape in higher pick densities. This, in return, leads to less moment of inertia of the section and thus less rigidity (B=EI) of the yarn. Lower rigidity of the yarn leads to higher deflection of the weft yarn. This transformation is severe at high pick densities. The flattening effect of weft and warp yarns in higher pick densities can be observed clearly in Fig. 4.

## 5 Conclusion

The deflection of weft in a plain woven fabric was studied. The weft was modeled as a fixed-fixed elastic beam deflected at the middle by normal load. Using the small deflection equations, the maximum deflection of weft was calculated. The normal load, causing the deflection of weft, was estimated using pullout test. The rigidity of fabric was measured and then the rigidity of weft yarn was calculated using the fabric specifications. The image of the actual shape of deformation of weft yarn in fabric was also obtained using microscope. The shape of actual bent weft in the fabric was compared to the theoretical deflection curve based on the small deflection modeling. The results show an acceptable agreement between actual curve and theoretical deflection curve. It can be concluded that fixed-fixed beam in small deflection case is useful for rapid computation and estimation of the deflection of weft in a plain woven fabric with an acceptable accuracy.

## References

1   Yu W & Du Z, *Text Res J*, 76(9) (2006) 702.
2   Afrashteh S, Merati A A & Jeddi AAA, *Indian Fibre Text Res*, 38 (2) (2013) 126.
3   Hasani H & Behtaz, S, *Indian Fibre Text Res*, 38 (1) (2013) 101.
4   Wei M & Chen R, *J Text Inst*, 85(3) (1994) 359.
5   Lomov S V, Truevtzer A V & Cassidy C, *Text Res J*, 70(12) (2000) 1088.
6   Ghosh T K & Zhou N, *Indian Fibre Text Res,* 28 (4) (2003) 471.
7   Ghane M, Azimpour I & Hosseini Ravandi S A, *Int Clothing Sci Technol*, 23(5) (2011) 310.
8   Hosseini Ravandi S A & Toriumi K, *J Text Inst*, 87(3) (1996) 522.
9   Kirkwood K M, Kirkwood J E, Lee Y S, Egres R G (Jr), Wetzel E D & Wagner N J, *Text Res J*, 74(10) (2004) 920.
10  Seo M H, Realff M L, Pan N, Boyce M, Schwartz P & Backer S, *Text Res J*, 63(3) (1993) 123.
11  Realff M L, Boyce M C & Backer S, *Text Res J*, 67(6) (1997) 445.
12  Bilisik K, *Text Res J,* 83(1) (2013) 13.
13  Bilisik K, *J Indust Text,* 41(3) (2012) 201.
14  Nash W A, *Schaum's Outline of Theory and Problems of Strength of Materials*, 4th edn (McGraw-Hill, New York, NY), 1998.
15  Szablewski P & Kobza W, *Fibers Text Eastern Eur*, 11(4) (2003) 54.
16  Kocik M, Zurek W, Krucinska I, Gersak J & Jakubczyk J, *Fibers Text Eastern Eur*, 13(2) (2005) 31.
17  Ghane M, Sheikhzadeh M, Halabain A M & Khabouri S, *Fibers Text Eastern Eur*, 16(3) (2008) 30.
18  Leaf G A V, Chen Y & Chen X, *J Text Inst*, 84(3) (1993) 419.
19  Valizadeh M, Hosseini Ravandi S A, Salimi M & Sheikhzadeh M, *J Text Inst*, 99(1) (2008) 47.